Recombination and Exchange Reactions of Hydrogen and Dihydrogen Molecular Condensation in Single-Walled Carbon Nanotubes

Yueyuan Xia,*,†,§ Mingwen Zhao,† Feng Li,† Boda Huang,‡ Zhenyu Tan,‡ Xiangdong Liu,† Yanju Ji,† and Liangmo Mei†

Department of Physics, Shandong University, Jinan, Shandong, 250100 P. R. China, Department of Optoelectronics, Shandong University, Jinan,Shandong, 250100 P. R. China, and State Key Laboratory of Crystal Materials, Shandong University, Jinan, 250100 P. R. China

Received: February 11, 2004

The hydrogen recombination reaction, $H + H \rightarrow H_2$, and the hydrogen exchange reaction, $H + H_2 \rightarrow H_2 + H$, taking place inside single-walled carbon nanotubes have been studied by using quantum mechanics molecular dynamics simulations. Two types of hydrogen exchange reactions have been found. The fast reaction lasts in less than 5 fs, and the slow one lasts for about 40 fs with a clear intermediate state manifested. The collisional reaction for two H atoms to form a H_2 molecule usually takes place in a time interval of 25 fs. We also describe the detailed process of the reaction of individual H atoms to form H_2 molecules and, with an increase of the density of H_2 molecules confined in the tubes, H_2 molecular condensation to form clusters and finally to form condensed H_2 molecular lattices.

Introduction

The hydrogen exchange reaction, $H + H_2 \rightarrow H_2 + H$, or the isotope variant of hydrogen exchange reaction, $H + D_2 \rightarrow HD + D$, has been studied extensively in recent years,[1−8] as this prototype reaction can shed light on the chemical dynamics details for molecular reactions. Meanwhile, formation of H_2 molecules on graphite or carbonaceous surfaces has attracted much interest to obtain a better understanding of the mechanism of abundant H_2 molecules found in the interstellar medium.[9−11] Hydrogen recombination on a graphite surface is also an important subject related to controlled fusion devices such as tokamaks.[12,13] However, all the investigations of the hydrogen exchange reaction, either experimental or theoretical, are relevant to the reaction in free space. Hydrogen recombination reactions are studied only for the cases of taking place on graphite or other material surfaces.[9−13] These reactions have not been systematically studied for the case of being confined in nanometer-scale spaces. Molecular reactions in a confined environment of single-walled carbon nanotubes (SWNTs) are particularly interesting for understanding various mechanisms such as gas adsorption and desorption, phase separations, capillary condensation, and surface-driven phase transitions.[14,15] Molecules confined within narrow carbon nanotubes with straight pore width of a few molecular diameters can exhibit a wide range of physical behavior. Through the studies of these prototype hydrogen reactions confined in SWNTs one can obtain a general understanding for more complex molecular reactions in confined nanoscale spaces. Besides the basic physical and chemical interest, hydrogen reaction and hydrogen confined in nanotubes have promoted extensive studies of hydrogen storage in carbon nanotubes in exploring pollution-free energy storage medium.[16,17] The phase transition studies of confined hydrogen molecular system in SWNTs may be helpful for further studies of synthesis novel one-dimension (1D) materials and for exploring the technological applications for various strain states of encapsulated 1D materials with tailor-able properties. Here, we report the results of hydrogen recombination and exchange reactions taking place inside single-walled carbon SWNTs, obtained by using quantum mechanics molecular dynamics simulations (QMMDS). At the present time, it is impossible to observe experimentally hydrogen exchange and recombination reactions inside nanotubes. Computer simulations for these reactions in nanoscale spaces may be the best method to provide intrinsic mechanism for these reactions in the confining environment. Therefore we use the QMMDS method to study these reactions in SWNT. We also describe the detailed process of individual H atoms reaction to form H_2 molecules, H_2 molecular condensation to form clusters, and finally to form condensed H_2 lattices.

Theoretical Methods

A (5, 5) SWNT segment with length ∼1.72 nm was used as a model tube. Each tip of the tube was capped with a hemisphere of C_{60} to form a (5, 5) tube capsule. Then we simulated the process of a H atom colliding at energy 20 eV on the side wall of the SWNT by using a QMMDS computer code, FIREBALL, based on the self-consistent density functional theory (DFT) tight-binding method.[18−20] It was found that under the collision condition the H atom was injected into the SWNT capsule and was confined inside the tube. This result agrees with our previous classical MDS study, which indicated that hydrogen atoms colliding, in the collision energy range 16−20 eV, onto the sidewalls of SWNTs had a high probability of being injected and confined inside the SWNTs.[21] The injected hydrogen atom traveled, with its residual kinetic energy, along a spiral trajectory turning from one tip to the other and continuing to transfer kinetic energy to the SWNT and gradually slowing down. When it lost most of its kinetic energy, it was adsorbed on the interior wall of the SWNT capsule. When we continued to inject more hydrogen atoms consecutively, different reaction events were

* Corresponding author. E-mail: yyxia@sdu.edu.cn.
† Department of Physics.
‡ Department of Optoelectronics.
§ State Key Laboratory of Crystal Materials.

10.1021/jp049370q CCC: $27.50
Published on Web 03/23/2004

observed. For examples, the adsorbed H atom was desorbed by collision with a moving hydrogen atom. Two encountering hydrogen atoms at collision energy higher than ~5 eV in center-of-mass frame, scattered from each other. Recombination reactions were observed when two slower hydrogen atoms collided with each other. Hydrogen exchange reactions were also observed when a reaction product, a H_2 molecule, collided with a hydrogen atom. We found that a single H atom in the SWNT, no matter whether it was a new injected one or was a product of the exchange reaction or desorbed H from the interior wall of the SWNT, could not exist for a long time. It usually collided with other H atoms to form a more stable H_2 molecule. The nanometer confining space made the collision frequency very high. In such a collisional environment, the adsorbed H atoms were usually desorbed by collision with other H atoms to join the new recombination reaction or exchange reaction to form a H_2 molecule. Therefore, the most stable products confined in SWNT are H_2 molecules.

In the present work we focus first on the recombination reactions and the exchange reactions observed in the (5, 5) SWNT capsule. To follow the recombination reaction, we selected randomly two H atoms that were approaching each other to commence a recombination reaction and followed their trajectories. In a similar way, when a hydrogen atom was found to approach to a H_2 molecule to induce an exchange reaction, we followed the trajectories of the reactants and the products. The model (5, 5) SWNT used is long enough for studying of these reactions because the recombination reaction and the exchange reaction are very rapid, usually in an interval of less than 70 fs, and the collision energies are usually less than 2 eV. To reduce the influence of the tube tips on the trajectories of the reactants, during the interval of the reaction taking place the caps on the tips were removed, and instead, the carbon atoms on the tips were saturated with hydrogen atoms. At each time step the spatial structures of the reactants and the products were observed. Meanwhile, the electron densities around the reactants and the products were obtained from the density matrix of DFT calculations. By using a projection program developed in our group, the electron density from the density matrix was projected on the reaction plane to obtain the electron density contour on the reaction plane at each time step.

To assign the vibration and rotational quantum states for the H_2 molecules before and after the exchange reaction, the detailed vibration and rotation data were analyzed. The rovibrational quantum states for the H_2 molecule before the reaction, (v, j), and for the nascent product H_2 molecule, (v', j'), were determined by equating the vibration internal energy of the H_2 molecule to $(v + {}^1/_2)\hbar$ for the initial H_2 molecule or to $(v' + {}^1/_2)\hbar$ for the nascent H_2 molecule, and equating the square of the classical rotational angular momentum modulus to $j(j+1)\hbar^2$ for the initial H_2 molecule or to $j'(j'+1)\hbar^2$ for the nascent H_2 molecule, respectively. The noninteger v, j, v', and j' values were then rounded to the nearest integer, respectively. This assignment method is the same as that used in ref 8.

The second focus of our study is the condensation process when the density of H_2 molecules confined in the SWNT capsule is increased beyond a critical value by increasing the number of injected hydrogen atoms. To study the H_2 molecular condensation process in a detailed manner, we switched the simulation from the QMMDS to classical MDS. There are three reasons for using a classical MDS method instead of QMMDS to simulate the condensation process. The first is that the condensation and relevant phase transitions are thermodynamic process, and the simulation time needed must be long enough, at least on the order of nanoseconds. The supercell used ought to be large enough. It is difficult to use QMMDS to simulate the detail process. The second, which may be more noticeable, is that the dominant interactions among the molecules involved in the condensation process are van der Waals interactions. If QMMDS methods were used, one ought to use a very accurate base set including polarization functions and diffusion functions and accurate exchange and correlation interactions should be used. This makes the QMMDS more impracticable. In addition, quantum mechanics consistent calculations do not allow us to add any empirical parameters, such as the Lennard-Jones form parameters to describe van der Waals molecular interactions. This explains why it is not commonly believed that the van der Waals interaction can be described correctly by using ordinary QMMDS, except for certain simple systems.[22] The third is that there has been a realistic empirical interaction potential, Brenner potential, that describes carbon and hydrocarbon systems accurately.[23,24] The van der Waals interactions have been incorporated into this potential expression.[25] We used this bond order potential to simulate the condensation process of H_2 molecules confined in a (5,5) SWNT capsule. In this case we used a much longer, ~3.5 nm, (5, 5) SWNT segment to form a model tube capsule. The hydrogen injection process was the same as that used in ref 21. To test if this classical simulation can give results consistent with those of the QMMDS, we also used the classical MDS to simulate the recombination and exchange reactions using the same supercell and the same collision conditions as those used in the QMMDS. We found that there were some differences in cohesive energy and bond length between the values predicted by the QMMDS and those predicted by the classical MDS. For example, the cohesive energy and the average bond length for carbon on the SWNT are −7.8 eV per atom and 1.45 Å, respectively, predicted by the QMMDS code, whereas these values predicted by the classical MDS are −7.4 eV per atom and 1.42 Å, respectively. The average bond length of the H_2 molecule predicted by the QMMDS is ~0.83 Å in comparison with ~0.74 Å predicted by the classical MDS. The differences reflect the difference potential surfaces involved in these computer codes, and in turn these will affect the trajectories of the reactants and the products. Nevertheless, all the reactions, as described above, predicted by the QMMDS were also observed by using the classical MDS. Therefore, the results obtained from the classical MDS and that from the QMMDS are reasonably consistent. In the next section we will report the main results of the study.

Results and Discussion

As described above, when a single H atom is injected into the SWNT capsule via collision, it travels along a spiral trajectory and is gradually slowing down by transferring its kinetic energy to the SWNT. This case is shown in Figure 1a, which simulates, by use of the QMMDS code, the trajectory of a hydrogen atom injected from the sidewall of the SWNT capsule by collision at 20 eV. In this figure, the large gray balls represent the carbon atoms on the wall of the tube, whereas the trajectory of the hydrogen atom at various time steps is shown by the smaller light gray balls with the spiral curve and arrows to indicate the head and the end of the trajectory in the time interval. Figure 1b shows that this injected H atom (the white ball) is adsorbed on a carbon atom (the black ball) on the wall. When another energetic H atom (the light gray ball) approaches the adsorption site, it moves around the adsorption site and is then scattered away, whereas the adsorbed H atom is desorbed. The arrows in this figure indicate the directions of motion of

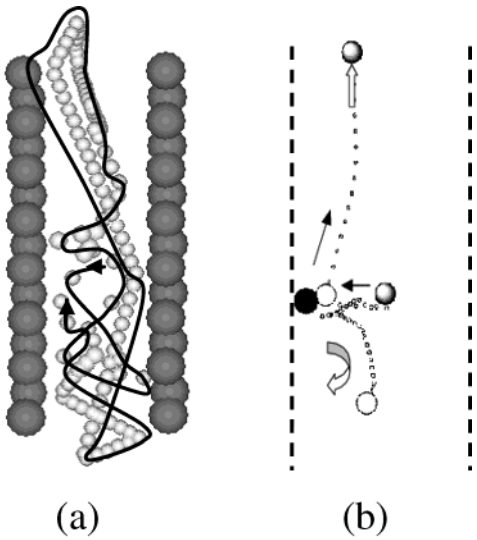

Figure 1. Trajectories of hydrogen atoms confined in a (5, 5) SWNT capsule: (a) trajectory of an injected H atom; (b) trajectories of a desorbed H atom (the white ball), from an adsorption site of a carbon atom (the black ball) on the wall of the SWNT, caused by collision with an incident H atom, that is scattered away (the gray ball).

the scattered H atom and the desorbed H atom, respectively, whereas the dashed lines show schematically the position of the wall of the SWNT. These hydrogen atoms will join the other collision reactions. Increasing the number of injected hydrogen atoms, the recombination reactions and exchange reactions are easy to observed. To analyze these reactions, both the coordination data of the reactants and the products and the electron density data of the whole system are recorded. These data are used to obtain the spatial structures of the reactants and the products and the corresponding electron density around them at each time step. Figure 2 shows the electron density contours on the reaction plane for a recombination reaction process obtained at 6 typical time steps. These contours were obtained from the density matrix data projected on the reaction plane containing hydrogen atoms A and B and the mass center of the SWNT. From this figure it is obvious that when hydrogen atoms A and B approach each other, their wave functions overlap, inducing a recombination reaction at $t = 430$ fs. At $t = 450$ fs, the reaction is completed by forming a H_2 molecule. This reaction takes place within a time interval ~25 fs. Both the reactant H atoms and the H_2 molecule formed have their electron cloud overlapped with that of the SWNT. Depending on how adjacent to the carbon atoms on the SWNT, the electron distribution around the particles has shapes that are different from those of H atom and H_2 molecule in free space. For example, at time $t = 426$ fs, atom A approaches atom B, which is very close to the wall of the tube and the influence of the carbon atoms on atom B can be clearly seen from the severe distortion of the electron cloud around it. Because the contour is drawn on the reaction plane and the angle between this plane and the plane containing atom B and its carbon neighbors is large, the carbon atom centers cannot be seen in the figure. Similarly, at time steps $t = 430$ fs, $t = 450$ fs, $t = 480$ fs, and $t = 500$ fs, the reaction product, the H_2 molecule, always brings the distorted electron cloud, resulting from the influence of the carbon atoms of the global system, traveling in the confined space. Only at $t = 460$ fs when the nascent H_2 molecule locates near the center of the SWNT, where the influence of the carbon atoms is weaker, can one find the H_2 molecule having an electron cloud similar to that of H_2 in free space. In this context, the recombination reactions, as well as the exchange reactions

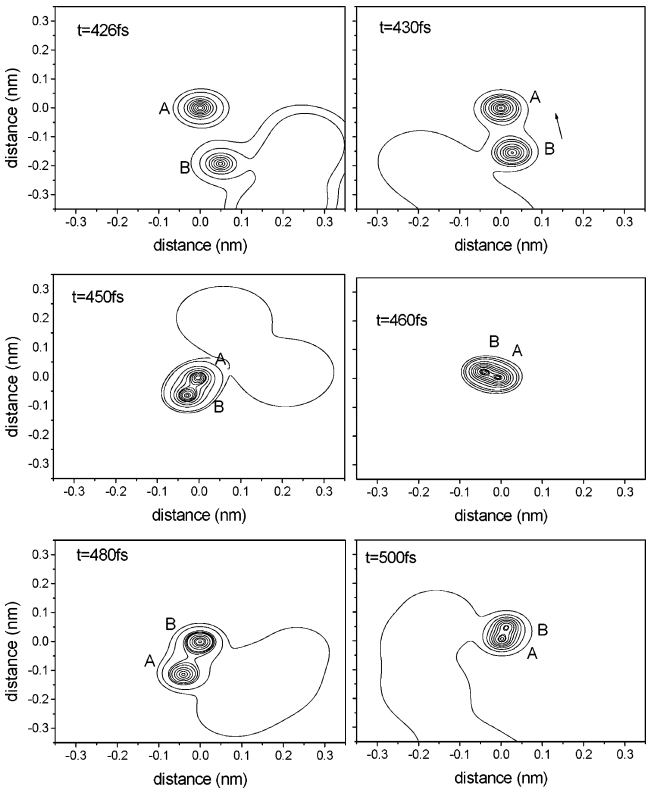

Figure 2. Snapshots obtained from the QMMDS for two H atoms collision to form a H_2 molecule, showing the electron density contours around the reactants and the product at 6 typical time steps.

to be analyzed later, studied in the nanoscale confined space are different from those in free space or reactions near the interfaces between surfaces and vacuum.

After the H_2 molecule is formed, it shows clearly the feature of rotational and vibrational excitation, as shown by the changing molecular length and axial orientation at $t = 460$ fs, $t = 480$ fs, and $t = 500$ fs, respectively. The vibration quantum number, v, and the rotational quantum number, j, for the nascent H_2 molecule are assigned as H_2 ($v = 1$, $j = 3$) by using the method mentioned in last section.

In searching for the exchange reactions, we follow the trajectories of a H_2 molecule, formed by the recombination reaction or other exchange reaction, and a hydrogen atom when they approach each other to induce an exchange reaction. Figure 3 depicts the snapshots of a rapid exchange reaction, H (A) → H_2 (BC) → H_2 (AC) + H (B). The electron density contours on the reaction plane containing atoms A, B, and C at four typical time steps are given in this figure. The vibration and rotational state of the H_2 (BC) before collision is H_2 ($v = 1$, $j = 3$). It is easy to understand the existence of this excited state because the H_2 is a product of a recombination reaction under the energetic collision condition. In fact, the experimental study of hydrogen exchange reaction at collision energy ~1.6 eV in ref 7 by using PHOTOLOC (photoinitiated reaction analyzes via the law of cosines) technique, they have found that the reagent, the hydrogen isotopic variant, D_2, having rotational quantum state distributed in $j = 0$, 1, and 2. As shown in this figure, at $t = 7.5$ fs, a hydrogen atom (A) and the H_2 molecule (BC) approach each other at collision energy $E = 1.21$ eV and at impact parameter $b = 0.17$ nm to induce an exchange reaction. At $t = 8.25$ fs, a transient state of A−C−B is observed. This transient state lasts for only a few femtoseconds, and at $t = 12.5$ fs a H_2 molecule (AC) is formed while the H (B) atom is detached. At $t = 17.5$ fs, the nascent H_2 (AC) is excited to a

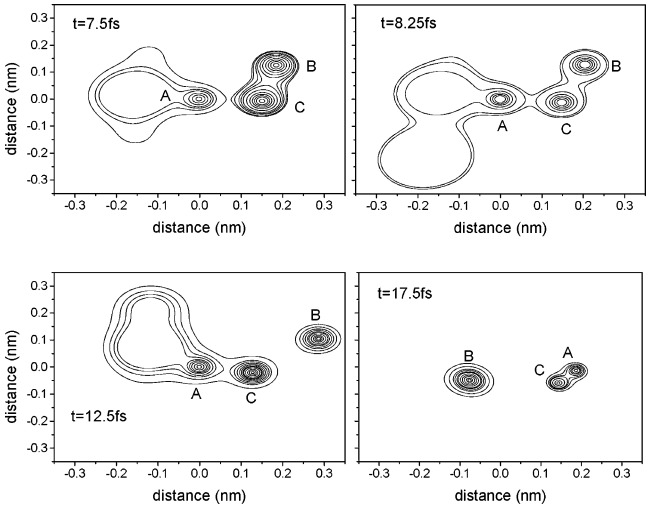

Figure 3. Snapshots obtained from the QMMDS of the hydrogen exchange reaction, showing the rapid exchange reaction happened within 5 fs.

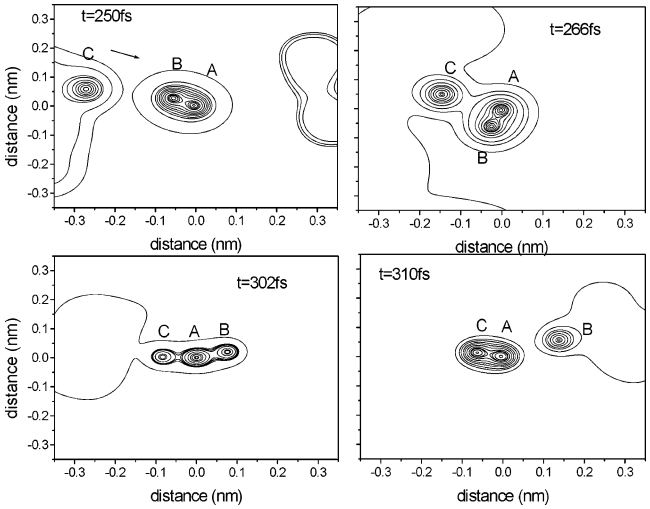

Figure 4. Snapshots obtained from the QMMDS of the hydrogen exchange reaction, showing the slow exchange reaction with an intermediate complex state formed.

vibration and rotational state H_2 ($v' = 2$, $j' = 6$), and the detached H (B) atom is further going away. This rapid exchange reaction takes place within 5 fs and it is obviously a direct reaction. However, this transient structure is not in a collinear shape, as the rapid exchange reaction reported in refs 1 and 6, where a direct recoil mechanism (H−H bonds breaking and forming concertedly while the system passes over a collinear transient state with recoil from the collision causing the H_2 product molecule to scatter backward) was used to explain the direct reactions taking place in free space. The direct recoil reactions usually take place at zero or low impact parameter and at low collision energy.[5,6] However, the impact parameter, $b = 0.17$ nm, for the exchange reaction shown in Figure 3 is large, a high rotational excited product H_2 molecule with $j' = 6$ is therefore obtained. This result is consistent with the experimental results of ref 5, which indicated that large impact parameter collision leads to high rotational excitation of the product. From the transient state existing in the time interval $t = 8.25$ fs to $t = 12.5$ fs shown in this figure, we find that this rapid exchange reaction occurs through a glancing collision, which involves angular momentum transfer and concerted bonds formation and breaking, with a rovibrational excited H_2 molecule produced. It is clearly distinguished from the slow exchange reaction that we have observed and will be analyzed.

Figure 4 shows the snapshots of a slow exchange reaction. At $t = 250$ fs, a H_2 molecule (AB) at vibration and rotational state H_2 ($v = 1$, $j = 3$) and a H (C) atom are colliding at energy $E = 1.50$ eV and at impact parameter $b = 0.24$ nm. At $t = 266$ fs, an A−B−C complex is formed. This intermediate complex changes its shape continuously. At $t = 302$ fs, it becomes a linear-like configuration, and until $t = 310$ fs it dissociates forming a H_2 (AC) molecule at vibration and rotational state H_2 ($v' = 1$, $j' = 1$) and a H (B) atom. This latter exchange reaction has several features that are different from the former one. The lifetime of the latter is about 40 fs and that of the former is less than 5 fs. This time delay ∼35 fs is comparable with that obtained in free space for the indirect exchange reactions involving the formation of H_3 intermediates reported by Althorpe[1] (∼25 fs) and that reported in ref 6 (∼15−35 fs). However, in refs 1 and 6 the results were obtained for the case of assuming the initial H_2 molecule to be at rovibrational ground state, H_2 ($v = 0$, $j = 0$). In the present QMMDS, we have chosen randomly the initial H_2 state from the products of the earlier hydrogen recombination reactions. Therefore, the initial H_2 molecules are at rovibrational excited states. In practice, H_2 molecules in a collisional environment are usually at excited states.[9,10] The reaction cross section of the exchange reaction obtained from rovibrational excited state has been found substantially different from that obtained from the rovibrational ground state.[26] In this context, the present QMMDS results for this prototype exchange reaction are more physically and chemically appealing. Another difference between the rapid and slow exchange reactions is that the former has the newly formed H_2 ($v' = 2$, $j' = 6$) being at a rovibrational excited state higher than that of the initial H_2 ($v = 1$, $j = 3$) molecule, whereas the latter has the newly formed H_2 ($v' = 1$, $j' = 1$) at an excited state lower than that of the initial H_2 (v=1, j=3). This rotational cooled-product of exchange reaction has not been reported previously. In a general comparison of these two exchange reactions observed in the SWNT with those observed in a vacuum,[1−8] we find that though the basic characters of the indirect or slow exchange reaction are similar in these different environments, the rapid exchange reaction found in the SWNT has properties different from those found in free space. Even if for the indirect exchange reaction, the rotational cooled H_2 product in SWNT has not been found in free space. The correlation of the different reactions with scattering angles, as that studied in free space,[1−8] cannot be informatively analyzed in the case of reactions in SWNT because the nanoscale confining space makes the collective contribution of the SWNT affect the trajectories of the reagents and the products. In addition, when we search for the exchange reaction trajectories, we have not found exchange reaction events occurring at zero or low-impact parameter, which may lead to rapid direct recoil reaction with collinear transient states. This situation was also found by using higher collision energy of 2.20 eV in free space.[8]

What is the final destination of the products of the reactions described above is another important subject worthy of studying. When the number of the H_2 molecules accumulated in the narrow tube is increased to an averaged linear density greater than ∼2.2 H_2/nm, H_2 molecules condensation will take place. The condensed phase of various species inside carbon nanotubes have been an excited subject for fundamental physics and chemistry to study the novel one-dimensional (1D) behavior and exploring the technological applications for various strain states of encapsulated 1D materials with tailorable properties.[15,27]

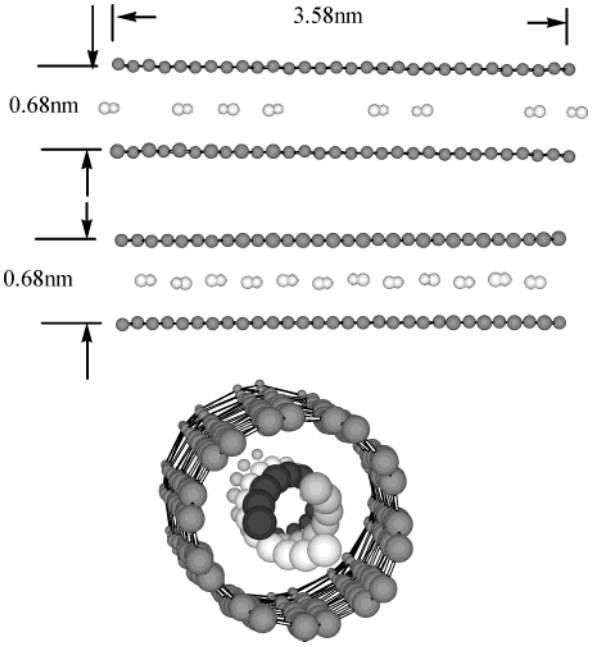

Figure 5. Small H_2 clusters and one-dimensional H_2 molecular lattices formed inside a (5, 5) SWNT at temperature, $T = 0.1$ K.

The condensation process can even take place at room temperature at a higher linear density of H_2 inside the SWNT. To see the structure of the condensed phase more clearly at low temperature, we use a Langevin MDS scheme,[28,29] which combines simulated annealing with molecular-dynamics calculation, to cool the system to low temperature. The top panel of Figure 5 shows the H_2 molecules condensed in the (5,5) SWNT at temperature, $T = 0.1$ K, when the linear density of H_2 reaches 2.3 H_2/nm. It is obvious that the H_2 molecules in the tube condensed to small clusters, each of which consists of a few H_2 molecules with their molecular axes aligned parallel to the tube axis. When the linear density increases to ~3.4 H_2/nm at $T = 0.1$ K, one observes a uniform 1D lattice, as shown in the middle panel of Figure 5. When the linear density of the H_2 molecules rise to ~12.2 H_2/nm, we obtain a quasi-1D lattice consisting of three helix molecular strands, as shown in the bottom panel of Figure 5. To see the regular lattice strands more clearly, in the bottom panel we use different colors, white, gray, and black, respectively, to represent the mass centers of the H_2 molecules in different strands. From this figure, it is clear that, depending on the H_2 linear density confined in the SWNT, one observes different condensed phases, from small clusters to different structures of quasi-1D lattices, the shapes of which are essentially determined by van der Waals interactions involved in the system.[25]

In summary, we have successfully used the QMMDS to elucidate the detail collision recombination and exchange reaction mechanisms for hydrogen confined in narrow SWNTs. Combining the QMMDS with the classical MDS, we have studied the H_2 molecular condensation process. This is the first time we have followed the whole process of individual H atoms forming H_2 molecules via a recombination reaction, the rapid and slow exchange reactions with different characteristic times, H_2 molecular condensation to small clusters at low H_2 linear density, and different lattice structures formed at higher linear density. Because the method used to study these prototype reactions can also be applied to more complex reactions, it means that the nanometer-spatial of SWNTs provides an ideal mold for study of molecular reactions, 1D phase transitions, and exploration of novel 1D materials with tailorable properties.

Acknowledgment. This work was supported by the National Natural Science Foundation of China under grant nos. 10175038 and 10374059, by the National Key Program of Fundamental Research under grant no. G1999064502, and by the Ministry of Education of China under grant no. 20020422012. We thank Dr. J. P. Lewis for providing the computer code, FIREBALL.

References and Notes

(1) Althorpe, S. C.; Fernandez-Alonso, F.; Bean, B.D.; Ayers, J. D.; Pomerantz, A. E.; Zare, R. N.; Wrede, E. *Nature* **2002**, *416*, 67.
(2) D′mello, M.; Manolopoulos, D. E.; Wyatt, R. E. *J. Chem. Phys.* **1991**, *94*, 5985.
(3) Neuhauser, D.; Judson, R. S.; Kouri, D. J.; Adelman, D. E.; Shafer, N. E.; Kliner, D. A. V.; Zare, R. N. *Science* **1992**, *257*, 519.
(4) Schnieder, L.; Seekamp-Rahn, K.; Borkowski. J.; Wrede, E.; Welge, K. H.; Aoiz, F. J.; Bañares, L.; D'Mello, M. J.; Herrero, V. J.; Sáez Rábanos, V.; Wyatt, R. E. *Science* **1995**, *269*, 207.
(5) Fernández-Alonso, F.; Bean, B. D.; Zare, R. N. *J. Chem. Phys* **1999**, *111*, 1035.
(6) Aoiz, F. J.; Herrero, V. J.; Rábanos, V. S. *J. Chem. Phys.* **1992**, *97*, 7423.
(7) Fernández-Alonso, F.; Bean, B. D.; Zare, R. N.; Aoiz, F. J.; Bañares, L.; Castillo, J. F. *J. Chem. Phys.* **2001**, *115*, 4534.
(8) Wrede, E.; Schnieder, L.; Welge, K. H.; Aoiz, F. J.; Bañares, L.; Castillo, J. F.; Martinez-Haya, B.; Herrero, V. J. *J. Chem. Phys.* **1999**, *110*, 9971.
(9) Parneix, P.; Bréchignac, Ph. *Astron. Astrophys.* **1998**, *334*, 363.
(10) Gough, S.; Schermann, C.; Pichou, F.; Landau, M.; Čadež, I.; Hall, R. I. *Astron. Astrophys.* **1996**, *305*, 687.
(11) Rutigliano, M.; Cacciatore, M.; Biling, G. D. *Chem. Phys. Lett.* **2001**, *340*, 13.
(12) Ferro, Y.; Marinelli, F.; Allouche, A. *J. Chem. Phys.* **2002**, *116*, 8124.
(13) Ferro, Y.; Marinelli, F.; Allouche, A. *Chem. Phys. Lett.* **2003**, *368*, 609.
(14) Gelb, L. D.; Gubbins, K. E.; Radhakrishnan, R.; Sliwinska-Barkowiak, M. *Rep. Prog. Phys.* **1999**, *62*, 1573.
(15) Calbi, M. M.; Cole, M. W.; Gatica, S. M.; Bojan, M. J. Stan, G. *Rev. Mod. Phys.* **2001**, *73*, 857.
(16) Dillon, A. C.; Jones, K. M.; Bekkedahl, T. A.; Klang, C. H.; Bethune, D. S.; Heben, M. J. *Nature* **1997**, *386*, 377.
(17) Lee, S. M.; Lee, Y. H. *Appl. Phys. Lett.* **2000**, *76*, 2877.
(18) Lewis, J. P.; Glaesemann, K. R.; Voth, G. A.; Frisch, J.; Demkov, A. A.; Ortega, J.; Sankey, O. F. *Phys. Rev. B* **2001**, *64*, 195103−1.
(19) Sankey, O. F.; Niokleswki, D. J. *Phys. Rev. B* **1989**, *40*, 3979.
(20) Demkov, A. A.; Ortega, J.; Sankey, O. F.; Grumbach, M. P. *Phys. Rev. B* **1995**, *52*, 1618.
(21) Ma, Y.; Xia, Y.; Zhao, M.; Wang, R.; Mei, L. *Phys. Rev. B* **2001**, *63*, 115422−1
(22) Jeloaica, L.; Sidis, V. *Chem. Phys. Lett.* **1999**, *300*, 157.
(23) Brenner, D. W. *Phys. Rev. B* **1990**, *42*, 9458.
(24) Brenner, D. W.; Shenderova, O. A.; Harrison, J. A.; Stuart, S. J.; Ni, B. Sinnott, S. B. *J. Phys.: Condens. Matter* **2002**, *14*, 783.
(25) Xia, Y.; Zhao, M.; Ma, Y.; Liu, X.; Ying, M.; Mei, L. *Phys. Rev. B* **2003**, *67*, 115117−1.
(26) Kliner, D. A. V.; Adelman, D. E.; Zare, R. N. *J. Chem. Phys.* **1991**, *95*, 1648.
(27) Meyer, R. R.; Sloan, J.; Dunin-Borkowski, R. E.; Kirkland, A. I.; Novothy, M. C.; Bailey, S. R.; Hutchison, J. L.; Green, M. L. H. *Science* **2000**, *289*, 324.
(28) Biswas, R.; Hamann, D. R. *Phys. Rev. B* **1986**, *34*, 896.
(29) Chelikowsky, J. R. *Phys. Rev. B* **1992**, *45*, 12062.